Modeling Quantized Coefficients with Generalized Gaussian Distribution with Exponent $1/m$, $m = 2, 3, \ldots$

Robert Krupiński(✉)

Chair of Signal Processing and Multimedia Engineering,
West-Pomeranian University of Technology in Szczecin,
ul. 26-Kwietnia 10, 71-126 Szczecin, Poland
rkrupinski@wp.pl

Abstract. The different types of signals in the image and signal processing applications can be modeled with generalized Gaussian distribution (GGD). When limiting to the special cases, then the closed form equations can be determined. The special cases with the exponents $p = 2$ (Gaussian distribution), $p = 1$ (Laplacian distribution), $p = 1/2$ and $p = 1/3$ are considered in literature. In the article, more general approach for the exponents $1/m$, $m = 2, 3, \ldots$ is analyzed, which are related to the peaky shapes of GGD. The maximum likelihood method for a discrete random variable is derived for this subclass of distributions.

Keywords: Estimation · Generalized Gaussian distribution · Maximum likelihood method · Centroid reconstruction

1 Introduction

GGD has been used in many image and signal processing areas. It is very often applied to model the transform coefficients. The coefficients of DCT (Discrete Cosine Transform), WHT (Walsh-Hadamard Transform) and DST (Discrete Sine Transform) could be modeled with GGD [2]. The DCT coefficients are available in the current video and image compression standards (MPEG, JPEG). DCT is performed for a block 8×8. The estimation of the shape parameters of GGD is applied to DCT coefficients. When $C_{i,j}$ denotes a coefficient in i row and j column in the block 8×8 of DCT coefficients then the indexes of DCT coefficients $C_{i,j}$ vary $i, j \in < 0, 7 >$, where $C_{0,0}$ corresponds to DC coefficient. A table with the estimated power parameters for the "Cameraman" image was presented in [6], where the values were in the range 0.26–0.59. The values depends on the source image, where for the "Lenna" and "Barbara" images the distributions were more close to GGD 0.5 [9].

The tangential wavelet coefficients for compressing three-dimensional triangular mesh data were modeled with zero-mean GGD [10]. GGD was used in the image segmentation algorithm based on the wavelet transform [17]. Certain

A. Gruca et al. (eds.), *Man-Machine Interactions 5*,
Advances in Intelligent Systems and Computing 659, DOI 10.1007/978-3-319-67792-7_23

regular statistical properties of natural images to get the natural scene statistics (NSS) model were modeled with GGD and asymmetric GGD (AGGD) [19]. GGD was applied to approximate an atmosphere point spread function (APSF) kernel to propose the efficient method to remove haze from a single image [18]. A GGD based model to introduce more facial details into the initial image synthesis was constructed by Song *et al.* [15]. The stereoscopic image quality assessment was proposed in [11], where the statistical properties of the stereoscopic image of the reorganized discrete cosine transform (RDCT) subband coefficients were modeled with GGD.

Many methods have been designed to estimate the parameters of GGD. A comparison of different methods for the estimation of a shape parameter can be found in [16]. These methods are complex and the approximated approach was proposed in [5,8].

For $p \to \infty$, the GGD density function becomes a uniform distribution, and for $p \to 0$, $f(x)$ approaches an impulse function. Chapeau-Blondeau and Monir [1] considered another special case $p = 1/2$. More peaky case of GGD $p = 1/3$ was discussed in [6].

When the encoder applies the quantization, the information is reduced, and only quantized coefficients are available to the decoder. Thus, the modeling of coefficients distribution should be performed with a discrete density function. Having this discrete distribution model, the reconstructed coefficients can be modified with, for instance, the centroid reconstruction to reduce the loss of a signal.

The cumulative distribution of GGD, the probability density function of GGD, the estimator of discrete GGD based on the maximum likelihood (ML) method, the centroid reconstruction of GGD for an exponent $p = 1/2$ were presented in [9]. The same set of equations for GGD with an exponent $p = 1/3$ was shown in [6].

By assuming a source signal with GGD with a power parameter $p = 1/m$, the equations for the centroid reconstruction in a closed form can be obtained, whereas for a GGD model it cannot be done and the ML method of discrete GGD $p = 1/m$ requires the estimation of only one parameter.

The article is organized in the following manner. In Sect. 2 the continuous GGD $p = 1/m$ is presented and in Sect. 3 the discrete GGD $p = 1/m$ is discussed. In Sect. 4 the biased reconstruction of quantized coefficients assuming GGD $p = 1/m$ is introduced. The experimental results are presented in Sect. 5.

2 Continuous Density Function with Exponent $1/m$

Probability density function of the continuous random variable of GGD is [2,3]

$$f(x) = \frac{\lambda \cdot p}{2 \cdot \Gamma\left(\frac{1}{p}\right)} e^{-[\lambda \cdot |x|]^p}, \tag{1}$$

where $\Gamma(z) = \int_0^\infty t^{z-1} e^{-t} dt, z > 0$ [12], p is the shape parameter and λ is connected to the variance of the distribution.

The subclass of the density function of GGD with the exponents $p = 1/m$, $m = 2, 3, \ldots$ of the continuous random variable is

$$f(x) = \frac{\lambda}{2 \cdot m!} e^{-[\lambda \cdot |x|]^{1/m}}. \tag{2}$$

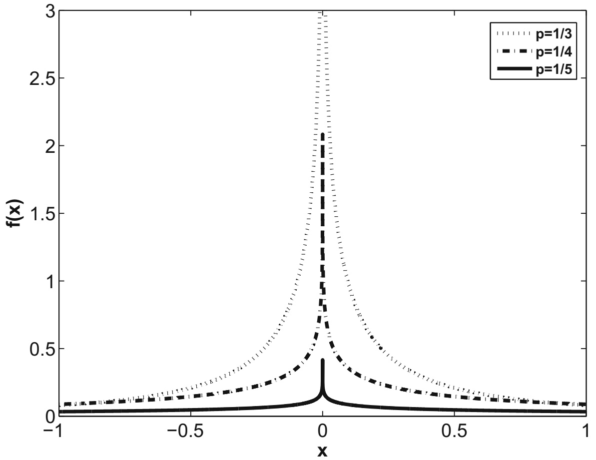

Fig. 1. Density function of GGD of the continuous random variable for the exponents $p = 1/3$, $p = 1/4$ and $p = 1/5$.

Figure 1 depicts the density functions of GGD of the continuous random variable for three selected parameters $m = 3$, $m = 4$ and $m = 5$.

The cumulative distribution is obtained by integrating (3)

$$F(x) = \int_{-\infty}^{x} f(z) dz, \tag{3}$$

which results in the cumulative GGD $p = 1/m$

$$F(x) = \begin{cases} A, & \text{for } x \leq 0 \\ 1 - A, & \text{for } x > 0 \end{cases}, \tag{4}$$

where

$$\begin{aligned} & c = (\lambda \cdot |x|)^{1/m}, \\ & \begin{cases} R(c,k) = c^k + k \cdot R(c, k-1) & k > 1 \\ R(c,1) = c + 1 & k = 1 \end{cases}, \\ & A = \tfrac{\exp(-c)}{2 \cdot (m-1)!} \cdot R(c, m-1). \end{aligned}$$

The advantage of fixing the power parameter is that the cumulative GGD $p = 1/m$ can be presented in a closed form (4).

The ML estimator for continuous GGD $p = 1/m$ can be obtained by finding the maximum likelihood function of (2) and maximizing it with respect to λ. After certain transformations the estimator takes the form

$$\lambda = \left(\frac{1}{m \cdot N} \sum_{i=1}^{N} |x_i|^{1/m} \right)^{-m}, \tag{5}$$

where N denotes the number of observations.

The coefficients, before quantization available to the encoder, are usually modeled with a probability density function of the continuous zero-mean random variable.

3 Discrete Density Function with Exponent $1/m$

The coefficients, available to the decoder, are reconstructed to the bin center for the JPEG and MPEG standards. The reconstructed values are $y_i = i \cdot Q$, where i is both the quantized value and the bin index, Q is the quantization factor (the length of the interval) and y_i represents a reconstructed value.

The probability density function of the discrete random variable of GGD $1/m$ is received by integrating (2) over the interval $(Q \cdot i - 0.5 \cdot Q, Q \cdot i + 0.5 \cdot Q)$

$$P_i = \frac{\lambda}{2 \cdot m!} \int_{(i-0.5)\cdot Q}^{(i+0.5)\cdot Q} e^{-[\lambda \cdot |x|]^{1/m}} dx, \tag{6}$$

which gives

$$\begin{cases} P_i = \frac{1}{2\cdot(m-1)!} \cdot [e^{-g_i} \cdot R(g_i, m-1) - e^{-h_i} \cdot R(h_i, m-1)] & i \neq 0 \\ P_0 = 1 - \frac{\exp(-a)}{(m-1)!} \cdot R(a, m-1) & i = 0 \end{cases}, \tag{7}$$

where

$$\begin{aligned} a &= (0.5 \cdot \lambda \cdot Q)^{1/m}, \\ h_i &= (\lambda \cdot (|y_i| + 0.5 \cdot Q))^{1/m}, \\ g_i &= (\lambda \cdot (|y_i| - 0.5 \cdot Q))^{1/m}. \end{aligned}$$

Figure 2 depicts the density function of GGD with exponent $p = 1/5$ and $\lambda = 1$ for the discrete random variable (P_i (7)) and continuous random variable ($f(x)$ (2)).

The ML function of (7) is set and then it is maximized with respect to λ [6,9,14]. After some transformations the ML estimator of discrete GGD $1/m$ becomes

$$\frac{N_0 \cdot e^{-a} \cdot Q}{P_0} + \frac{1}{\lambda} \sum_{i=1}^{N_1} \frac{e^{-h_i} \cdot h_i^m - e^{-g_i} \cdot g_i^m}{P_i} = 0, \tag{8}$$

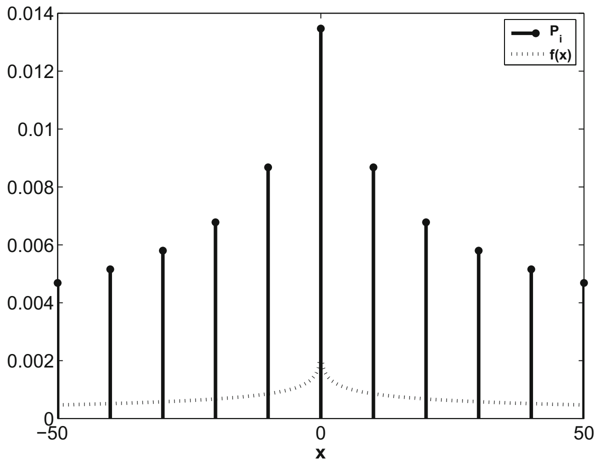

Fig. 2. Density function of GGD with the exponent $p = 1/5$ and $\lambda = 1$ for the discrete random variable (P_i (7)) and continuous random variable ($f(x)$ (2)).

where N_0 denotes the number of observations equal zero, N_1 denotes the number of observations not equal zero and $N = N_0 + N_1$.

The estimated λ parameter is received only from the discrete observations (the quantized values available to the decoder).

4 Centroid Reconstruction of Coefficients

The reconstructed coefficients can be modified to improve the quality of reconstructed signal. The reconstruction for the Laplace distribution with a centroid was presented in [7,14].

The application of the centroid reconstruction equation [13] for GGD $1/m$ gives

$$\hat{y}_i = sgn(y_i) \cdot \frac{1}{\lambda} \cdot \frac{L_i}{P_i}, \tag{9}$$

where

$$L_i = \frac{1}{2 \cdot (m-1)!} \cdot [e^{-g_i} \cdot R(g_i, 2 \cdot m - 1) - e^{-h_i} \cdot R(h_i, 2 \cdot m - 1)].$$

The value reconstructed with a centroid $\hat{y}_i$ minimizes the Mean Square Error (MSE) in the interval $(Q \cdot i - 0.5 \cdot Q, Q \cdot i + 0.5 \cdot Q)$.

It should be noted that the reconstruction equation can be presented in a closed form.

5 Experiments

In the first experiment, the continuous (5) and discrete (8) ML estimators of GGD $1/m$ are compared. The initial sequence is generated with the GGD generator [4] for $m = 4$. Then the sequence is quantized and dequantized, which corresponds to lossy compression. The dequantized coefficients are used as input observations for the estimators. The simulation was repeated 1000 times. Relative Mean Square Error (RMSE) was calculated from the equation

$$RMSE = \frac{1}{M}\sum_{i=1}^{M}\frac{(\hat{\lambda}-\lambda)^2}{\lambda^2}, \tag{10}$$

where $\hat{\lambda}$ is a value estimated by the model and λ is a real value from the generator. M denotes the number of repetitions.

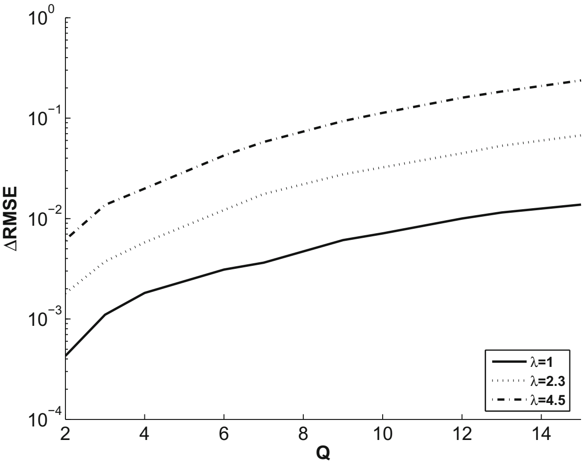

Fig. 3. Difference between RMSE of the estimators (5) and (8) for the sequence length $N = 1000$.

Figure 3 depicts the difference between RMSE of the continuous estimator (5) and discrete one (8) for $N = 1000$ and the selected λ values over varying a quantization factor. RMSE is higher in a value for the continuous estimator than RMSE of discrete one, so the difference between two $\Delta RMSE = RMSE_{cont} - RMSE_{discr}$ is a non-negative value (as in Fig. 3). The higher the difference is, the better the discrete estimator is. It can be noticed that the estimator based on the discrete distribution outperforms the estimator based on the continuous distribution and the RMSE difference increases with the increase of the quantization factor.

Figure 4 also confirms better performance of the discrete estimator for a varying sequence length.

In the next experiment, the DCT coefficients are generated with the GGD generator for $m = 4$. Then the inverse of DCT (IDCT) is calculated for them creating the input sequence x_i. The DCT coefficients are quantized and dequantized, and then the sequence z_i is calculated with IDCT. MSE is calculated for

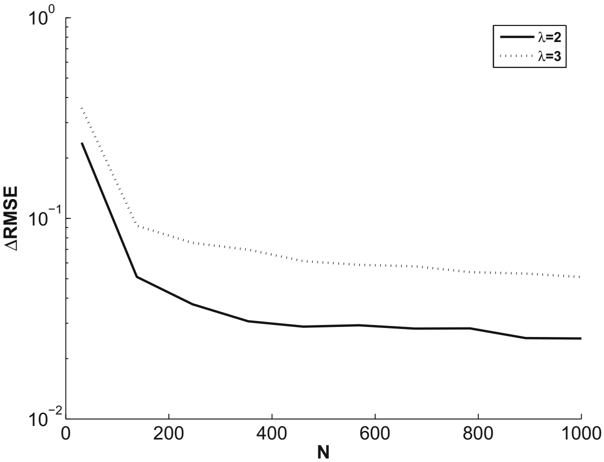

Fig. 4. Difference between RMSE of the estimators (5) and (8) for the quantization factor $Q = 10$.

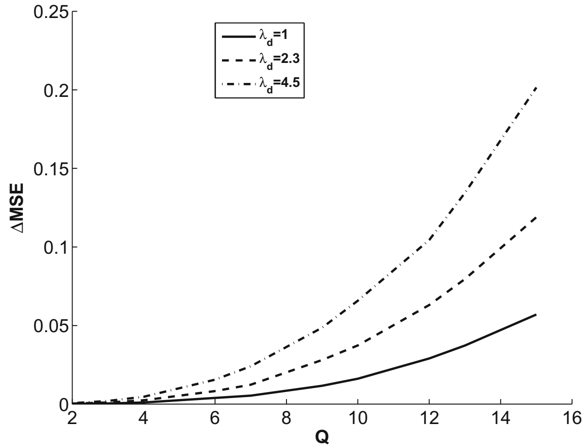

Fig. 5. Difference between MSE of normally reconstructed signal z_i and modified reconstruction $\hat{z}_i$ (9) for the sequence length $N = 1000$ (IDCT).

the reconstructed sequence z_i (or the modified reconstructed sequence $\hat{z}_i$) and the input signal x_i

$$MSE = \frac{1}{N} \sum_{i=1}^{N} (\hat{z}_i - x_i)^2. \tag{11}$$

The reconstructed DCT coefficients are modified according to (9) before IDCT.

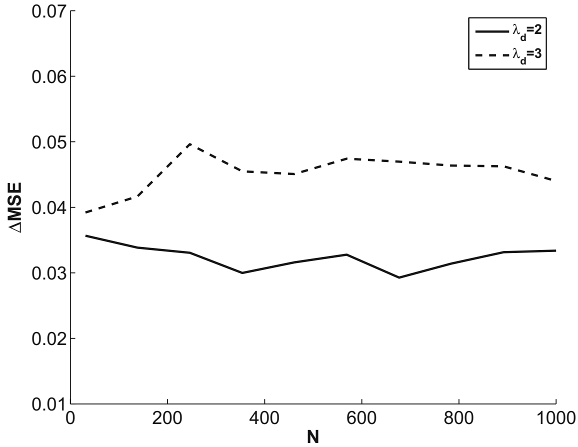

Fig. 6. Difference between MSE of normally reconstructed signal z_i and modified reconstruction $\hat{z_i}$ (9) for the quantization factor $Q = 10$ (IDCT).

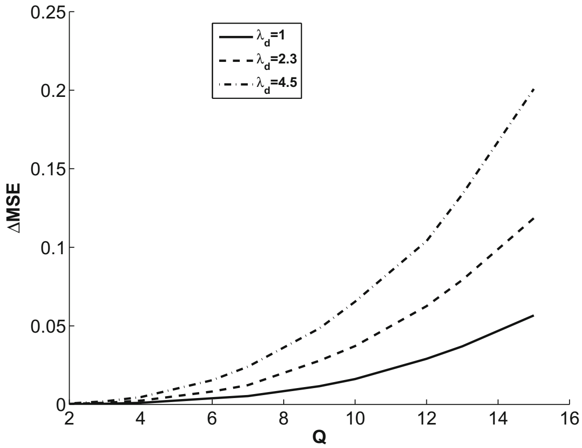

Fig. 7. Difference between MSE of normally reconstructed signal z_i and modified reconstruction $\hat{z_i}$ (9) for the sequence length $N = 1000$ (IDWT).

Figures 5 and 6 depict the difference between MSE of normally reconstructed signal z_i and modified reconstruction $\hat{z_i}$ (9). It can be noticed that the modified reconstruction $\hat{z_i}$ gives smaller MSE than MSE of normally reconstructed signal z_i.

In the last experiment, the detailed Discrete Wavelet Transform (DWT) coefficients are generated with the GGD generator for $m = 4$. Then the inverse of DWT (IDWT) is calculated for them (the approximation DWT coefficients are set to zero) creating the input sequence x_i. The DWT coefficients are quantized

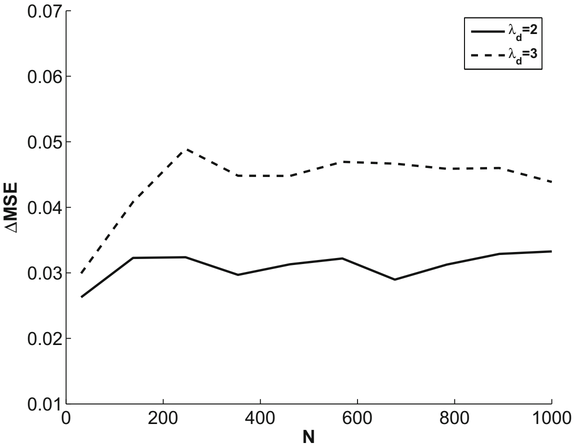

Fig. 8. Difference between MSE of normally reconstructed signal z_i and modified reconstruction $\hat{z}_i$ (9) for the quantization factor $Q = 10$ (IDWT).

and dequantized, and then the sequence z_i is calculated with IDWT. The reconstructed DWT coefficients are modified according to (9) before IDWT.

Figures 7 and 8 depict the difference between MSE of normally reconstructed signal z_i and modified reconstruction $\hat{z}_i$ (9). It should be noticed that the modified reconstruction $\hat{z}_i$ also gives smaller MSE than MSE of normally reconstructed signal z_i.

6 Summary

By setting $1/m$, $m = 2, 3, \ldots$ for the power parameter in GGD it becomes possible to denote the subclass of GGD with the cumulative distribution, the probability density function and the centroid reconstruction for GGD with a closed form equations. The discrete estimator based on the ML method for this GGD subclass has been derived. The simulations showed that MSE can be improved by the application of the modified reconstruction for the signals that are transformed with either DWT or DCT, where the information is lost by quantization.

References

1. Chapeau-Blondeau, F., Monir, A.: Numerical evaluation of the lambert w function and application to generation of generalized gaussian noise with exponent 1/2. IEEE Trans. Signal Process. **50**(9), 2160–2165 (2002)
2. Clarke, R.J.: Transform Coding of Images. Academic Press, New York (1985)
3. Du, Y.: Ein sphärisch invariantes verbunddichtemodell für bildsignale. Arch. Elektron. Übertragungstechnik AEÜ **45**(3), 148–159 (1991)

4. Kokkinakis, K., Nandi, A.K.: Exponent parameter estimation for generalized gaussian probability density functions with application to speech modeling. Sig. Process. **85**(9), 1852–1858 (2005)
5. Krupiński, R.: Approximated fast estimator for the shape parameter of generalized Gaussian distribution for a small sample size. Bull. Pol. Acad. Sci. Tech. Sci. **63**(2), 405–411 (2015)
6. Krupiński, R.: Reconstructed quantized coefficients modeled with generalized Gaussian distribution with exponent 1/3. Image Process. Commun. **21**(4), 5–12 (2016)
7. Krupiński, R., Purczyński, J.: First absolute moment and variance estimators used in JPEG reconstruction. IEEE Sig. Process. Lett. **11**(8), 674–677 (2004)
8. Krupiński, R., Purczyński, J.: Approximated fast estimator for the shape parameter of generalized Gaussian distribution. Sig. Process. **86**(2), 205–211 (2006)
9. Krupiński, R., Purczyński, J.: Modeling the distribution of DCT coefficients for JPEG reconstruction. Sig. Process. Image Commun. **22**(5), 439–447 (2007)
10. Lavu, S., Choi, H., Baraniuk, R.: Estimation-quantization geometry coding using normal meshes. In: DCC 2003, pp. 362–371. IEEE (2003)
11. Ma, L., Wang, X., Liu, Q., Ngan, K.N.: Reorganized DCT-based image representation for reduced reference stereoscopic image quality assessment. Neurocomputing **215**, 21–31 (2016)
12. Olver, F.W.J.: Asymptotics and Special Functions. Academic Press, New York (1974)
13. Paez, M.D., Glisson, T.H.: Minimum mean-square-error quantization in speech PCM and DPCM systems. IEEE Trans. Commun. **COM–20**, 225–230 (1972)
14. Price, J.R., Rabbani, M.: Biased reconstruction for JPEG decoding. IEEE Sig. Process. Lett. **6**(12), 297–299 (1999)
15. Song, C., Li, F., Dang, Y., Gao, H., Yan, Z., Zuo, W.: Structured detail enhancement for cross-modality face synthesis. Neurocomputing **212**, 107–120 (2016)
16. Yu, S., Zhang, A., Li, H.: A review of estimating the shape parameter of generalized Gaussian distribution ournal of Computational. J. Comput. Inf. Syst. **21**(8), 9055–9064 (2012)
17. Wang, C.: Research of image segmentation algorithm based on wavelet transform. In: ICCC 2015, pp. 156–160. IEEE, Chengdu (2015)
18. Wang, R., Li, R., Sun, H.: Haze removal based on multiple scattering model with superpixel algorithm. Sig. Process. **127**, 24–36 (2016)
19. Zhang, Y., Wu, J., Xie, X., Li, L., Shi, G.: Blind image quality assessment with improved natural scene statistics model. Digit. Sig. Process. **57**, 56–65 (2016)